

DOE/PC/94212--75

*Kinetics of Mn-Based Sorbents for Hot Coal Gas Desulfurization*

**Quarterly Progress Report** for the period of September 15 to December 15, 1995.  
Task 2: Exploratory Experimental Studies: Single Pellet Tests; Rate Mechanism Analysis

By  
M. T. Hepworth, Principal Investigator and Mr. Joseph Berns, Graduate Research Assistant,  
Department of Civil Engineering, University of Minnesota, Minneapolis, MN-55455.

December 15, 1995

Work Performed Under Grant: DE-FG-22-94PC94212

For:  
U.S. Department of Energy  
Pittsburgh Energy Technology Center  
Pittsburgh, PA 15236-0940

**DISCLAIMER**

This report was prepared as an account of work sponsored by an agency of the United States Government. Neither the United States Government nor any agency thereof, nor any of their employees, makes any warranty, express or implied, or assumes any legal liability or responsibility for the accuracy, completeness, or usefulness of any information, apparatus, product, or process disclosed, or represents that its use would not infringe privately owned rights. Reference herein to any specific commercial product, process, or service by trade name, trademark, manufacturer, or otherwise does not necessarily constitute or imply its endorsement, recommendation, or favoring by the United States Government or any agency thereof. The views and opinions of authors expressed herein do not necessarily state or reflect those of the United States Government or any agency thereof.

RECEIVED  
USDOE/PETC  
95 DEC 11 AM 9:59  
ADMINISTRATIVE SERVICES DIV.

DISTRIBUTION OF THIS DOCUMENT IS UNLIMITED

**MASTER**

## 1. INTRODUCTION

The Morgantown Energy Technology Center (METC) of the U.S. Department of Energy (DOE) is actively pursuing the development of reliable and cost-effective processes to clean coal gasifier gases for application to integrated gasification combined cycle (IGCC) and molten carbonate fuel cell (MCFC) power plants. A large portion of gas cleanup research has been directed towards hot gas desulfurization using Zn-based sorbents. However, zinc titanate sorbents undergo reduction to the metal at temperatures approaching 700 °C<sup>1,2</sup> and lose reactivity because of volatilization. In addition, sulfate formation during regeneration leads to spalling of reactive surfaces<sup>2,3</sup>.

Because of these problems with zinc-based sorbents, METC has shown interest in formulating and testing manganese-based sorbents. Westmoreland and Harrison evaluated numerous candidate sulfur sorbents and identified Mn as a good candidate<sup>4</sup>. Later, Turkdogan and Olsson tested manganese-based sorbents which demonstrated superior desulfurization capacity under high temperatures, and reducing conditions<sup>5</sup>. Recently, Ben-Slimane and Hepworth conducted several studies on formulating Mn-sorbents and desulfurizing a simulated fuel gas<sup>6</sup>. Although thermodynamics predicts higher over-pressures with Mn versus Zn, under certain operating conditions Mn-based sorbents may obtain < 20 ppmv as described in the previous quarterly report. In addition, the manganese-sulfur-oxygen (Mn-S-O) system does not reduce to the metal under even highly reducing gases at high temperatures (550-900 °C)<sup>4,6</sup>.

Currently, many proposed IGCC processes include a water quench prior to desulfurization. This quench is required for two reasons; limitations in the process hardware (1000 °C), and excessive Zn-based sorbent loss (about 700 °C). With manganese, the water quench is not necessary to avoid sorbent loss, since Mn-based sorbents have been shown to retain reactivity under cyclic testing at 900 °C<sup>7,8</sup>. This advantage of manganese over zinc has potential to increase thermal efficiency as the trade-off of increasing the equilibrium H<sub>2</sub>S over-pressure obtainable with a manganese sorbent. In the work which is reported here, lower loading temperatures (as low as 400 °C) are studied. Also formulations containing titania rather than alumina are studied to attempt to improve performance.

## 2. METHODS AND MATERIALS

In this report, formulation variables considered in preparing manganese-based sorbents included:

- MnO-to-substrate stoichiometric ratio (2:1 to 6:1).
- Manganese grade; a reagent  $\text{MnCO}_3$  and an ore  $\text{MnO}_2$ .
- Substrate; alundum and titania.
- Binder; weight percent bentonite (0-2%).
- Induration temperature ( $> 1100$  °C).

Feedstock designations and purities were listed in the previous quarterly report and are not repeated here. The chemical analysis of the formulations is given in Table 1. The formulations which report high in titanium, i. e., C6-2, C8-0 and C9-2 contain titania rather than alundum as the added substrate. The C-series pellets are made from manganese carbonate; whereas, the A-series originates from the ore source. The designation after the dash i. e., C4-2 represents the percent bentonite added. Samples C8-0 and A1-0 contain no bentonite binder. The assays in this table are in weight percent.

## 3. EXPERIMENTAL RESULTS

In Table 2, the results of mercury porosimetry testing is shown on freshly indurated pellets for some of the formulations. The designation after the second dash is for the induration temperature in degrees Centigrade, i. e., A1-2-1125 would be a pellet indurated for two hours at 1125 °C. Note that the pores coalesce and form much larger mean pore diameters and, as a result, less pore volume as the induration temperature is increased. The bulk density also decreased with increasing induration temperature. C6-2 and C9-2 differ in that the manganese-to-titanium mass ratio is somewhat lower in the former than the latter, i. e. 4.58 compared with 6.82. The carbonate-based pellets show superior performance with respect to pore diameter than the pellets which are ore-based (i. e., A1-2-1125).

Element	C4-2	C4-5	C5-2	C5-5	C6-2	C7-2	C8-0	C9-2	A1-0	A1-2	A2-2
Mn	51.6	48.0	57.5	52.7	54.6	37.1	48.7	58.6	50.0	47.8	50.1
Al	13.8	14.5	9.20	10.9	0.411	22.3	0.069	0.295	11.8	12.7	10.9
Ti	0.401	0.413	0.260	0.302	11.9*	1.08	19.1*	8.59*	0.745	0.802	0.316
Si	1.16	2.38	1.08	2.31	0.995	1.10	0.202	0.925	1.44	1.99	1.83
Fe	0.177	0.267	0.120	0.252	0.111	1.77	0.051	0.087	2.73	2.534	2.71
Ca	0.418	0.403	0.400	0.407	0.230	0.522	0.137	0.335	0.293	0.407	0.401
K	-	-	-	-	-	-	-	-	0.471	0.471	0.524

Table 1. Chemical Analysis of Freshly Indurated Pellet Formulations. \* Analysis for Ti approaching 10% by weight is qualitative.

Pellet Properties	Form A1-2-1125	Form C6-2-1100	Form C9-2-1110	Form C5-2-1250
Total Intrusion Volume, ml/g	0.2220	0.2328	0.1618	0.2901
Total pore area, sq-m/g	0.490	-----	0.199	0.103
Median pore diameter (volume), microns	4.7579	4.1741	4.1157	10.9701
Median pore diameter (area), microns	0.0142	-----	2.9058	10.0270
Average pore diameter (4V/A), microns	1.8116	-----	3.2474	11.3167
Bulk density, g/ml	-----	2.1073	2.4126	1.8807
Apparent (skeletal) density, g/ml	-----	4.1357	3.9580	4.1390
Porosity, percent	-----	49.05	39.05	54.56

Table 2. Results of Mercury Porosimetry tests of freshly indurated pellets made on PoreSizer 9320 (V2.04)

Figures 1-7 give the mechanical properties of the pellets. In Figure 1, the cumulative intrusion of mercury is given as a function of pressure as a measure of the pore diameter. The equivalent pore diameter in microns is shown on this plot. Smaller pores result from induration at lower temperatures, for example comparing C5-2-1250 vs. C6-2-1100, the lower induration temperature is seen to produce smaller pore diameters.

Figure 2 shows the incremental intrusion as a function of equivalent pore diameter. The median pore diameter are seen to be clustered around 4 to 4.5 except for the pellet formulation C5-2-1250 where the median pore diameter is about 10 microns. Therefore, the mean pore diameter is seen to be more dependent on the induration condition than the pellet composition. Similar effects are seen in Figures 3 through 4.

In Figure 5 the strength of the various formulations with titania and carbonate-based manganese is exhibited as a function of induration temperature. The threshold value for strength criteria was chosen as 3 pounds per mm of pellet diameter. All formulations are with titania except C5-2 which is with alumina for comparison. The formulation without binder (C8-0) requires temperatures above 1210 °C to achieve the required minimum strength; whereas, the other formulations achieve the requisite strength at lower temperatures.

In Figure 6 comparison of strength for manganese carbonate-based with alundum as a matrix material is compared as a function of induration temperature. From these plots, formulation C6-2 appears the best for high strength and lowest induration temperature.

In Figure 7, comparison is made between manganese-ore based material with alundum as a supporting matrix. These results are given to tie-in with prior work which was reported previously.

Figure 8 examines the reactivity of pellets as previously described using a sulfidizing atmosphere for pellets subjected to thermo-gravimetric analysis (TGA). The plots for the titania-matrix material (i. e. C6, C8, and C9 exhibit superior performance to C5, the alundum-matrix material. The comparison is not ideal since the pore sizes and induration conditions are not identical. The rapid rise seen initially is a result of surface reactivity; whereas, the more gradual rise after ten minutes is a result of sulfur diffusing into the pores of the pellet.

Figure 9 shows the effect upon reactivity and loading rate with decreasing temperature. The point to be noted is that pellets still retain significant reactivity to temperatures as low as 500 °C; however for temperatures of 400 °C the reactivity drops significantly.

Figure 10 exhibits the effect of prior induration temperature on the conversion rate. The goal is to achieve a high conversion rate with a strong pellet: two opposing goals which require optimization. Indurations for this formulation of 2 hours at 1100 °C appear to be satisfactory.

Figure 11 relates pellet diameter with reactivity showing, as expected, that smaller pellets are more reactive.

In Figure 12 the formulations indurated at the lower temperature, i. e. 1100 °C show higher capacities than the formulation indurated at 1230 °C.

Figure 13 compares alundum-based formulations with respect to pore size and induration temperature.

Figure 14 shows that higher manganese levels correlate well with increasing capacity, as would be expected.

Figure 15 compares the reactivity of the best formulations which were developed.

Figure 16 is a plot showing reduction, loading, regeneration followed by a repeat of the half cycle of reduction and loading. The sample chosen was for carbonate-based manganese with titania as a substrate and 2% bentonite. Areas B and E compare the loading cycles and show that, if anything, the rate of loading and conversion increases after the first cycle. This is consistent with previously reported work by Hepworth and Ben Slimane.

Figure 17 is a similar plot for another carbonate-based material with titania as a substrate and 0% bentonite.

Figure 18 shows results for an ore-based sample with no bentonite. Region D in this plot is higher than region D in the prior plot (carbonate-based material) indicating that some sulfur is tied up irreversibly with the gangue constituents of the ore-based material.

#### 4. CONCLUSIONS:

Carbonate-based manganese is more suitable than ore-based material since there is more manganese actively available for reaction and no gangue constituents to tie up sulfur in the sulfate form.

Titania appears to be superior to alumina as a substrate material probably because the manganese/titania bond is weaker than the manganese/alumina bond. This means that the manganese which is tied up in forming a spinel has a higher activity in the titania form than the alumina form and is more effective in reacting with sulfur.

Bentonite is helpful in increasing the strength of the pellet but tends to reduce its reactivity for a given induration condition.

It is possible to achieve high strength pellets without bentonite but at the cost of higher induration temperatures.

Strength and reactivity have opposed behavior with respect to induration temperature. One of the objectives of this program is to optimize this function. However, the induration campaigns were determined before the initiation of the reactivity tests. Induration temperature sensitivity is only reasonably optimized since pellet reactivity shows a quantitative change for induration temperature increments of 25 °C.

## 5. REFERENCES

1. Focht, G.D., et al, "High Temperature Desulfurization Using Zinc Ferrite: Reduction and Sulfidation Kinetics." *Chemical Engineering Science*, Vol. 43, No. 11, pp. 3005-3013, 1988.
2. Woods, M.C., et al, "Reaction between H<sub>2</sub>S and Zinc Oxide-Titanium Oxide Sorbents. 1. Single-Pellet Kinetic Studies." *Ind. Eng. Chem. Res.* 1990, Vol. 29, 7, pp.1160-1167.
3. Focht, G.D. et al. *Structural Property Changes In Metal Oxide Hot Coal Gas Desulfurization Sorbents*, DOE/METC (DE-AC21-84MC2166), 1986.
4. Westmoreland, P.R., and Harrison, D.P., "Evaluation of Candidate Solids for High-Temperature Desulfurization for Low-BTU Gases." *Environmental Science and Technology*, 1976, Vol. 10, pp. 659-651.
5. Turkdogen, E.T. and Olsson, R.G., "Desulfurization of Hot Reducing Gases with Manganese Oxide Pellets", *Proceedings of the Third International Iron and Steel Congress*, Chicago IL., Apr. 16-20, 1978, pp. 488-491.
6. Ben-Slimane, R., and Hepworth, M.T., "Desulfurization of Hot Coal-Derived Fuel Gases with Manganese-Based Regenerable Sorbents. 3. Fixed-Bed Testing", Accepted for publication in *Energy and Fuels*, March/April Issue, 1995.
7. Ben-Slimane, R., and Hepworth, M.T., "Desulfurization of Hot Coal-Derived Fuel Gases with Manganese-Based Regenerable Sorbents. 1. Loading (Sulfidation) Tests", *Energy and Fuels*, Vol. 8, 1994, pp. 1175-1183.
8. Gasper-Galvin, L., DOE/METC, personal correspondence, September 1995.
9. Ben-Slimane, R., and Hepworth, M.T., "Desulfurization of Hot Coal-Derived Fuel Gases with Manganese-Based Regenerable Sorbents. 2. Regeneration and Multicyclic Tests", *Energy and Fuels*, Vol. 8, 1994, pp. 1184-1191.
10. Ben-Slimane, R., PhD Thesis, University of Minnesota, 1994

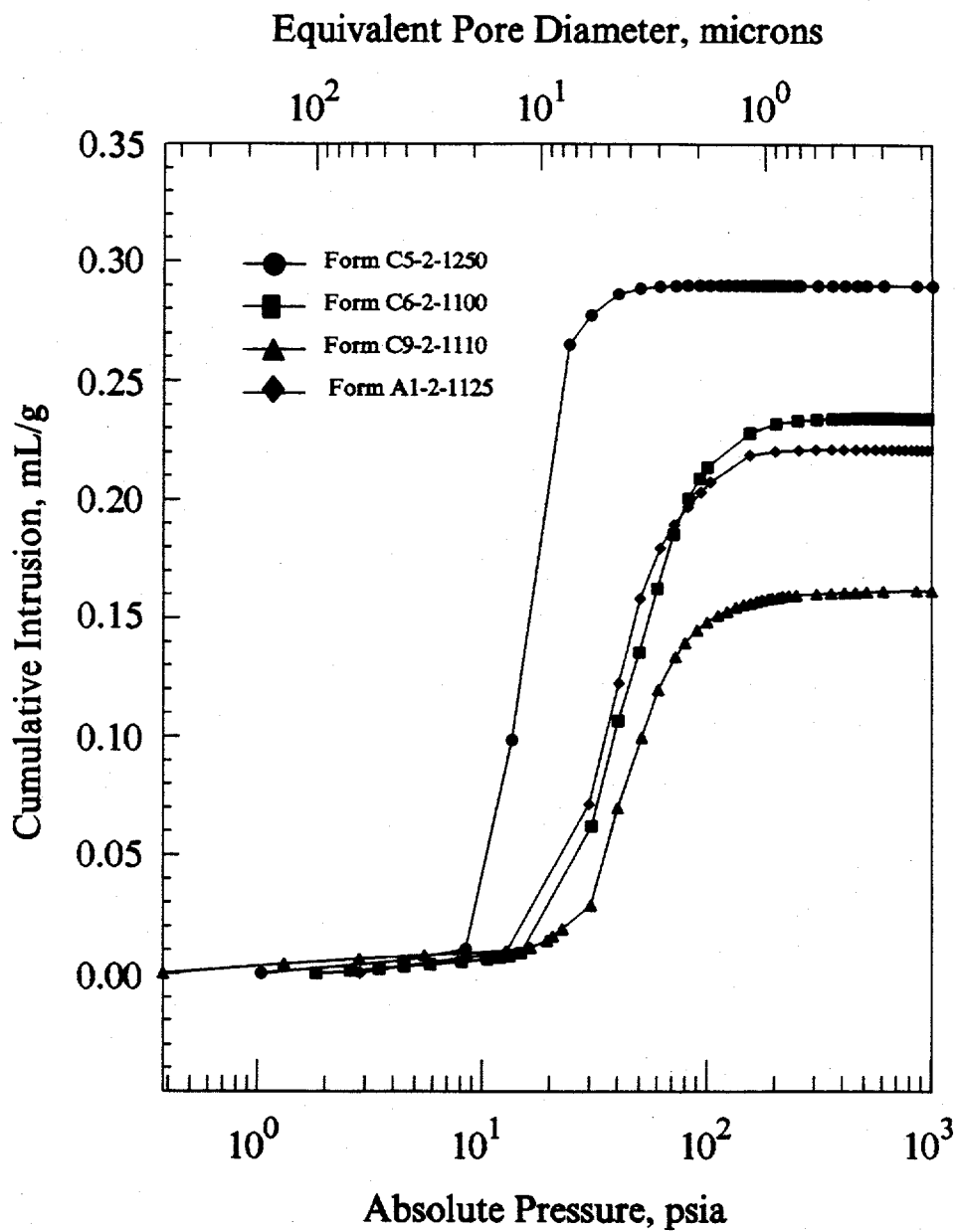


Figure 1. Cumulative intrusion as a function of pressure.

Results of Mercury Porosimetry Test of freshly indurated pellets.

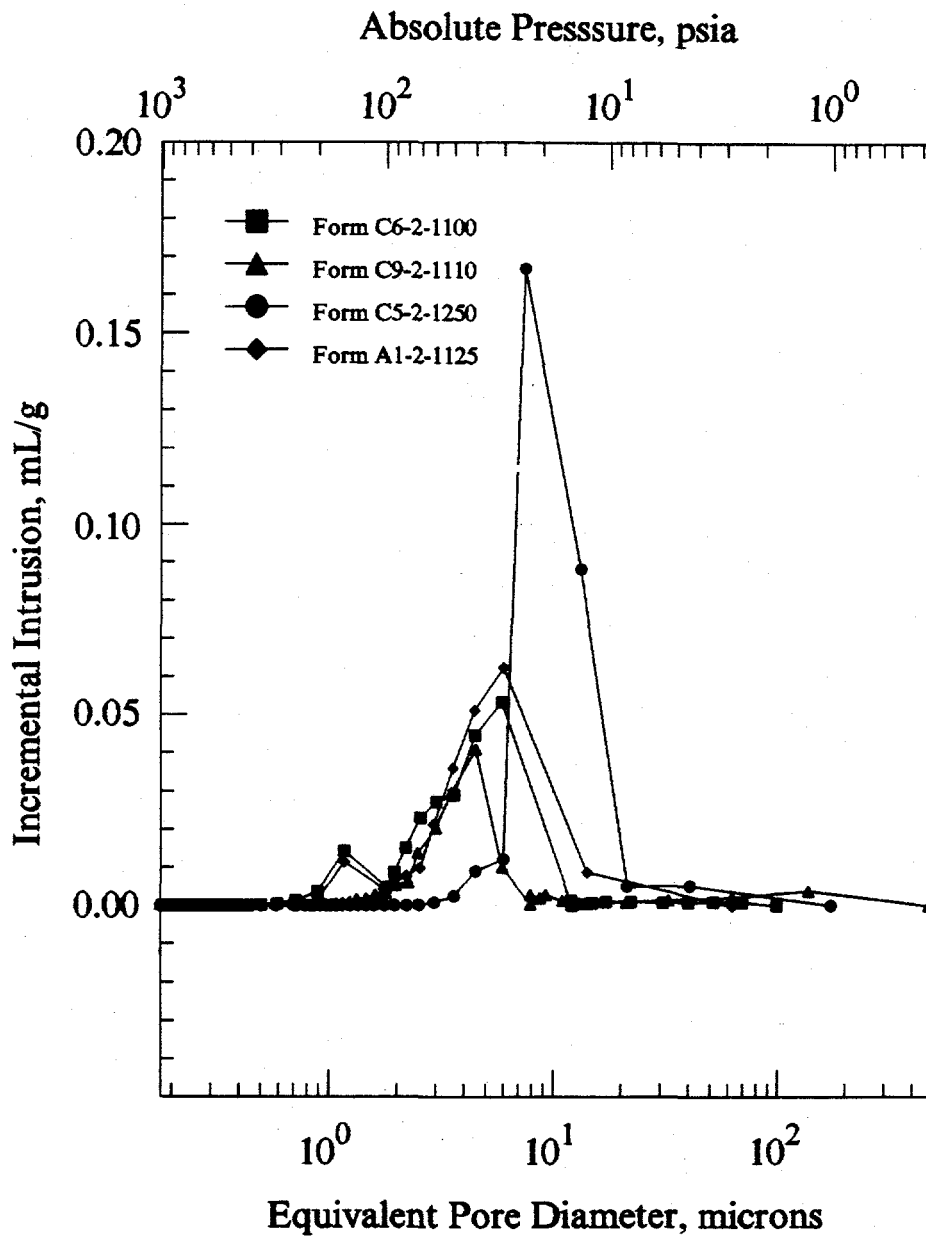


Figure 2. Incremental intrusion as a function of equivalent pore diameter.  
Results of Mercury Porosimetry Test of freshly indurated pellets.

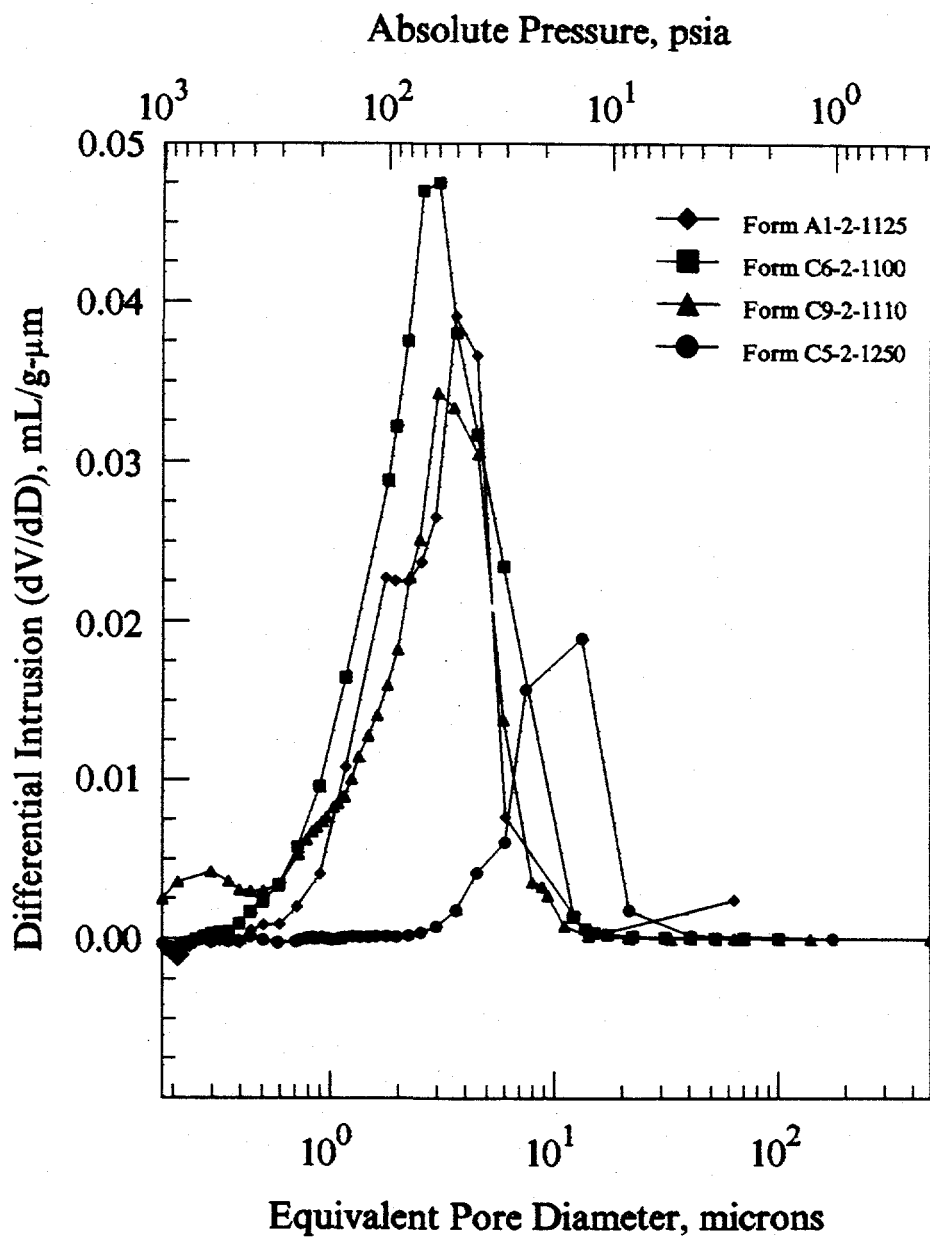


Figure 3. Differential intrusion as a function of equivalent pore diameter.  
Results of Mercury Porosimetry Test of freshly indurated pellets

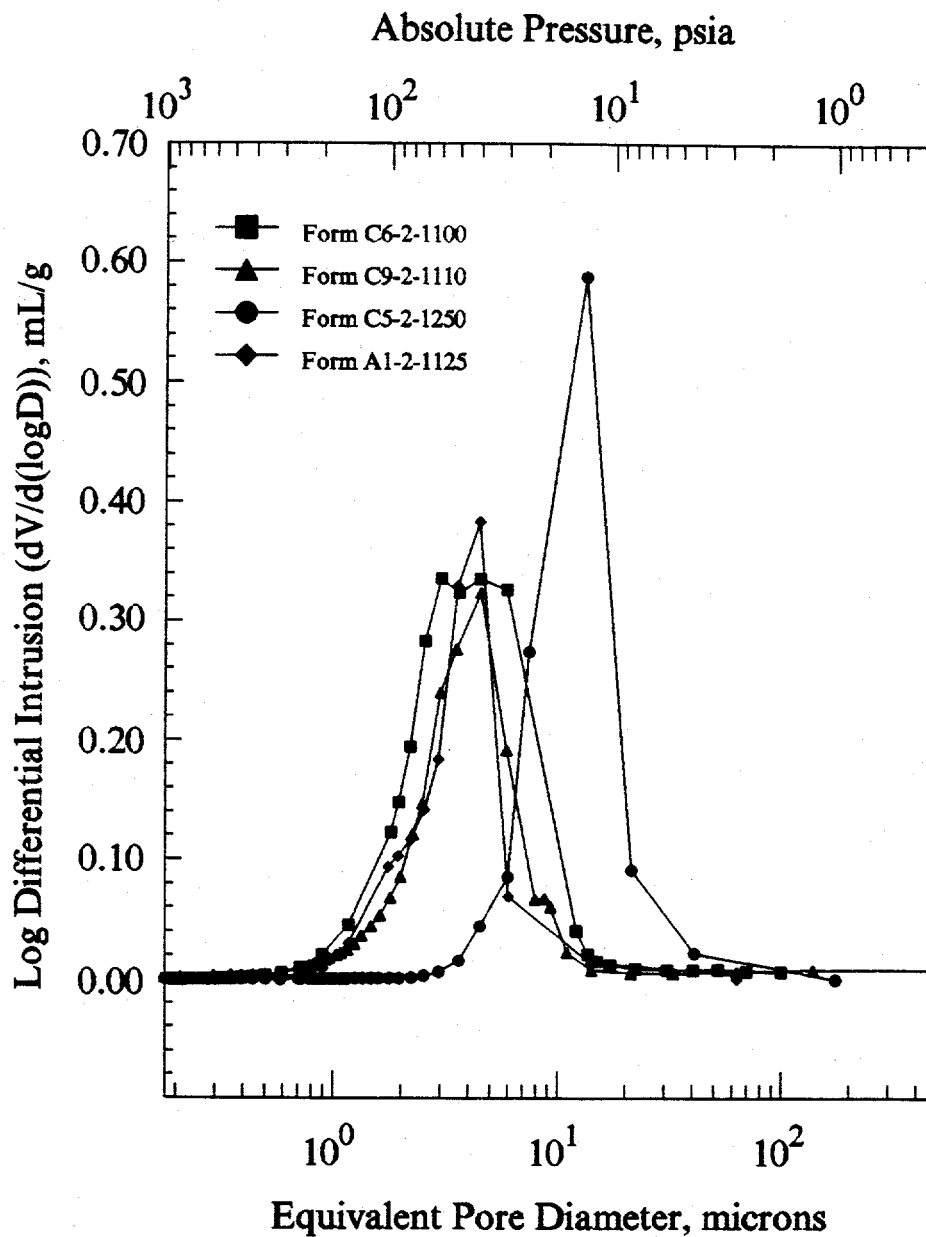
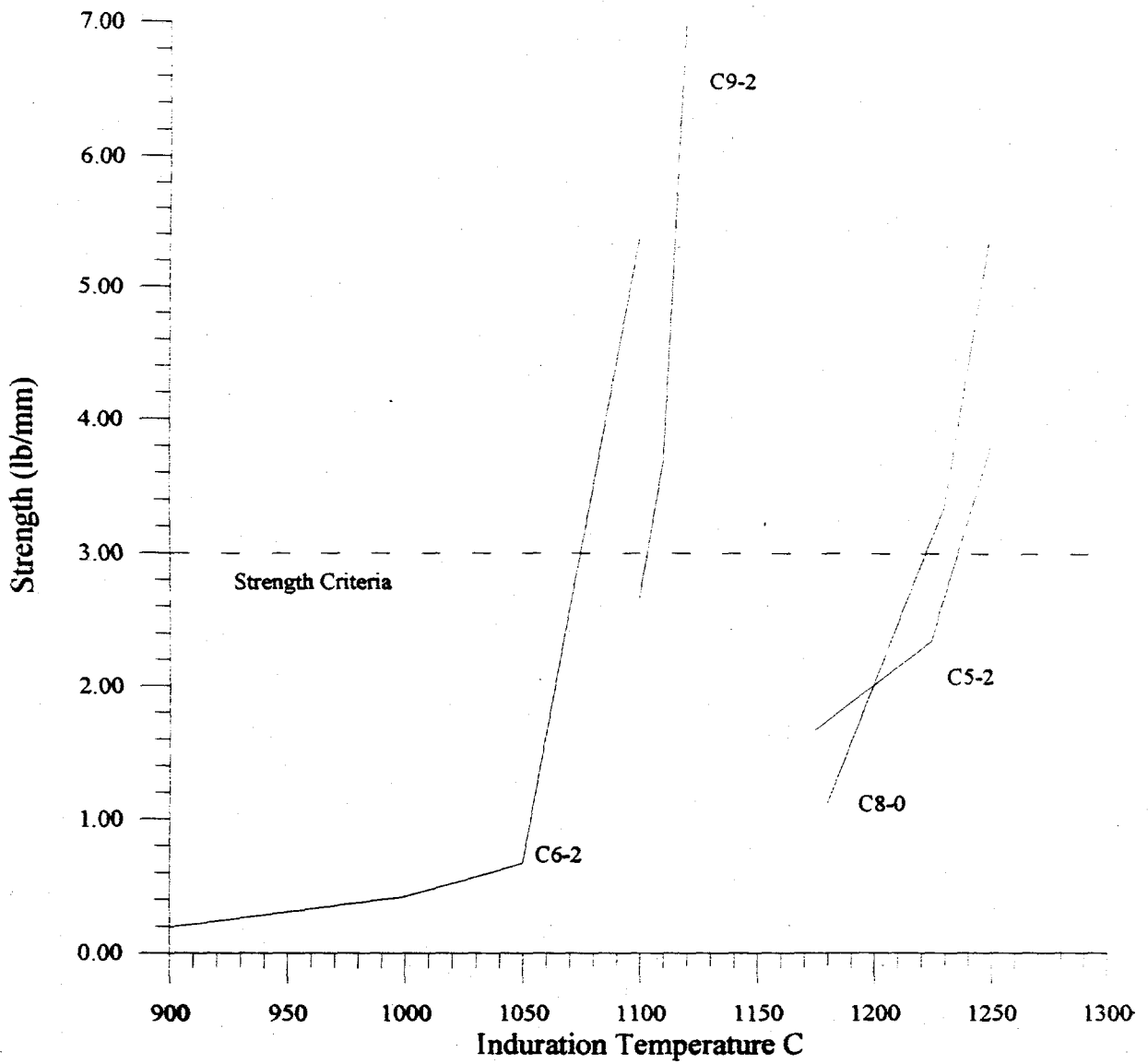


Figure 4. Logarithmic differential intrusion as a function of equivalent pore diameter. Results of Mercury Porosimetry Test of freshly indurated pellets.



**Figure 5.** Strength for various induration temperatures (Mn-carbonate based formulations with Titania as supporting matrix).

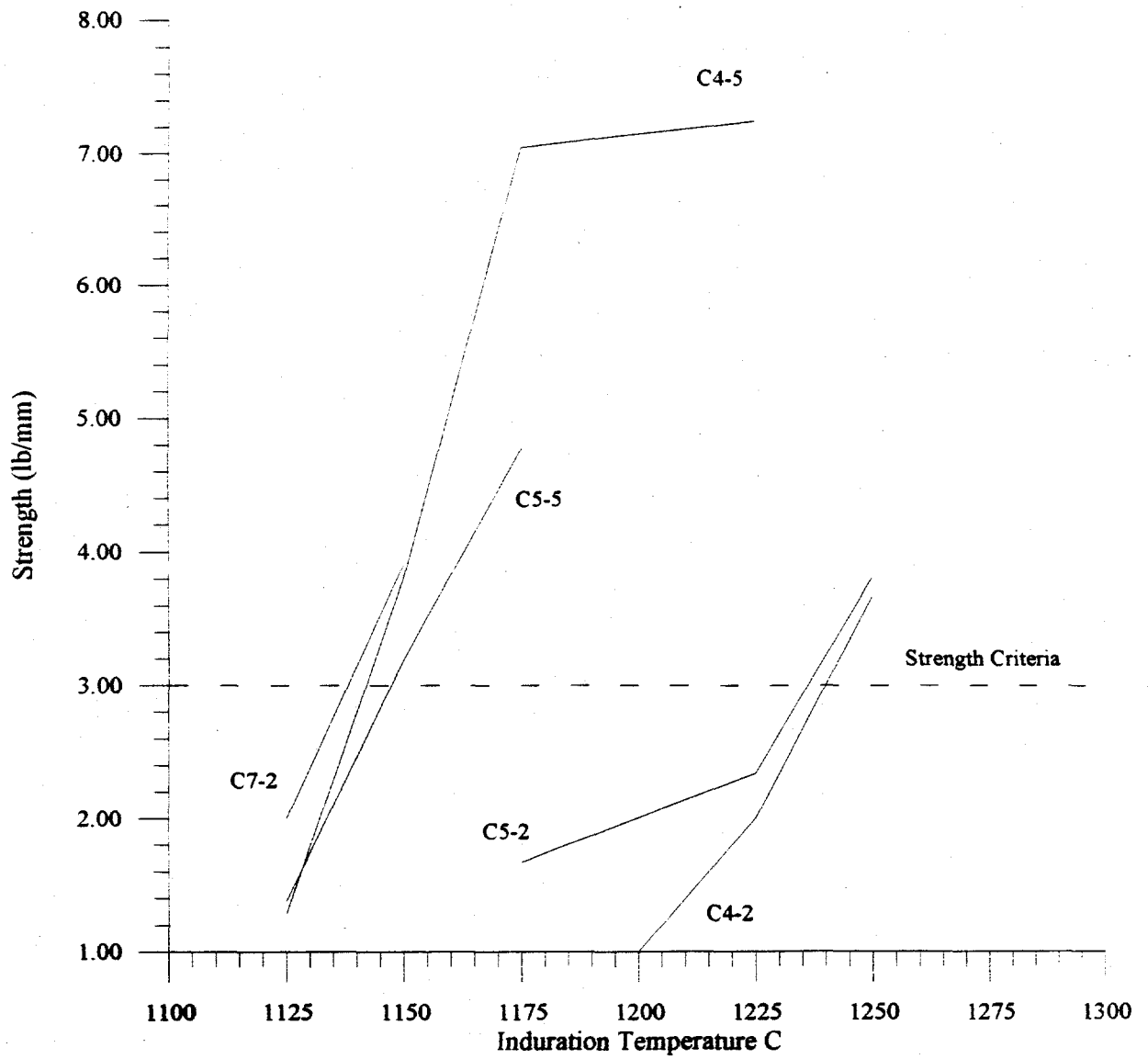


Figure 6. Strength for various induration temperatures (Mn-carbonate based formulations with Alundum as supporting matrix).

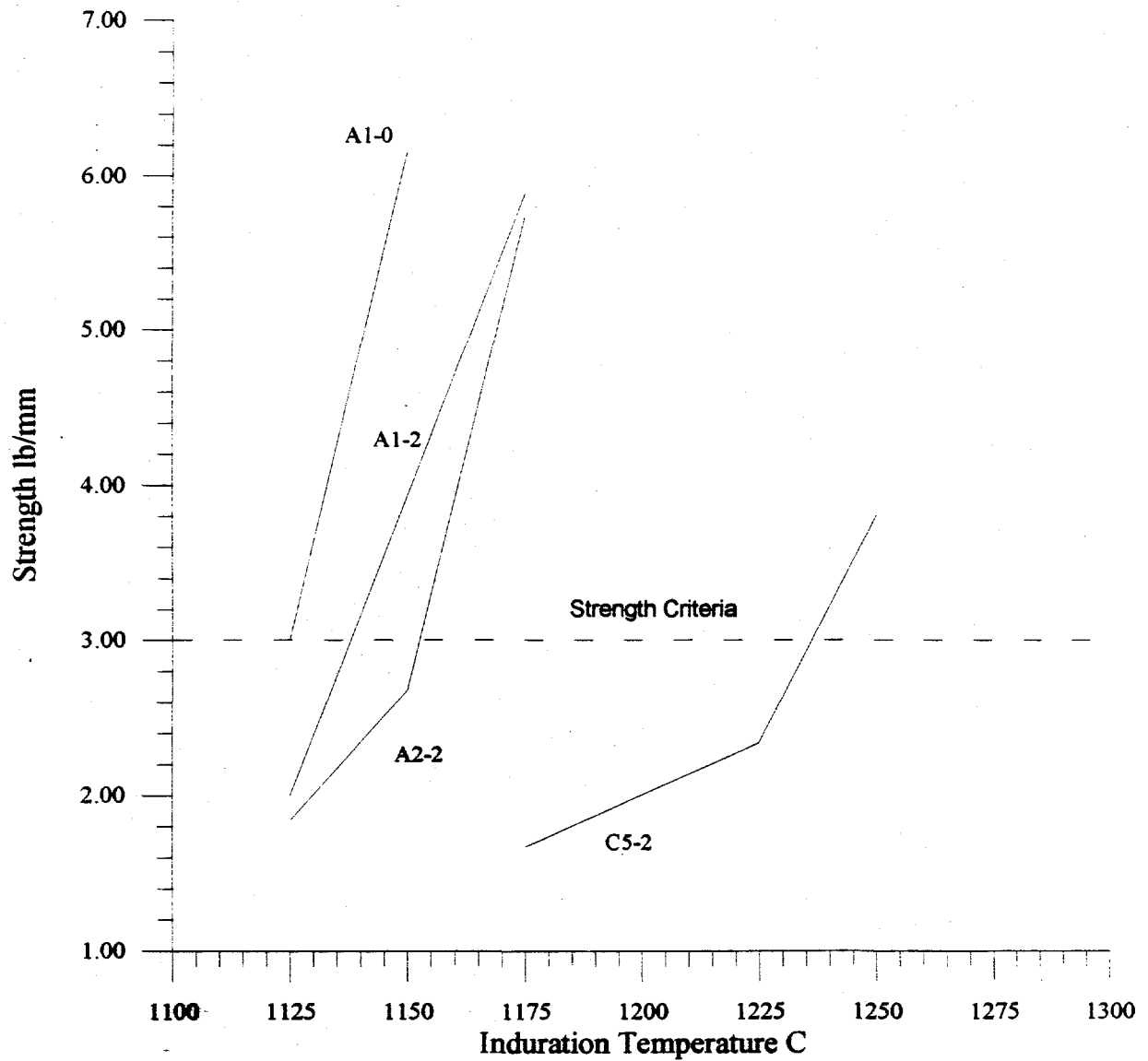


Figure 7. Strength for various induration temperatures (Mn-ore based formulations with Alundum as supporting matrix).

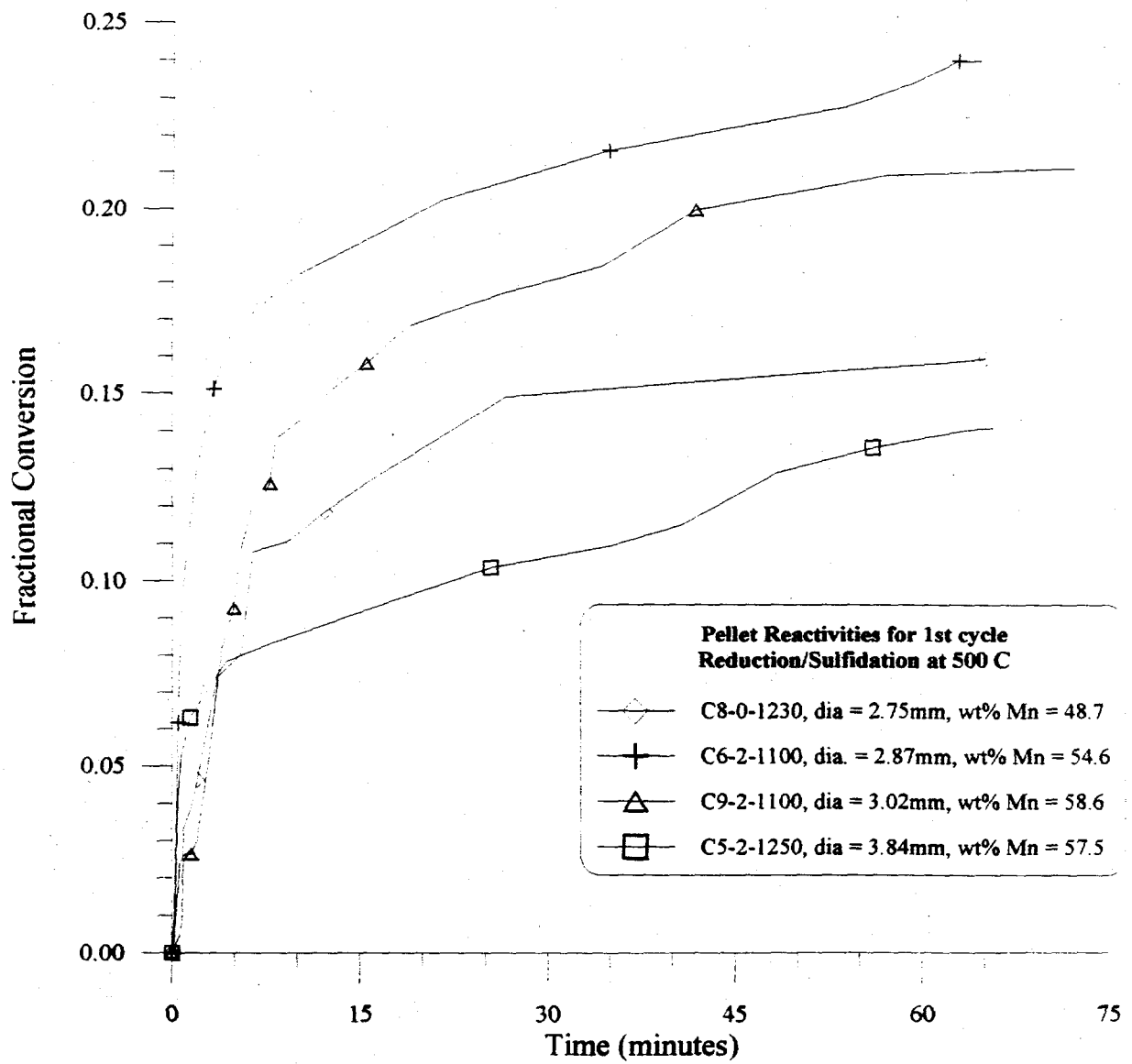


Figure 8. First cycle reactivity at 500 °C, for selected formulations.

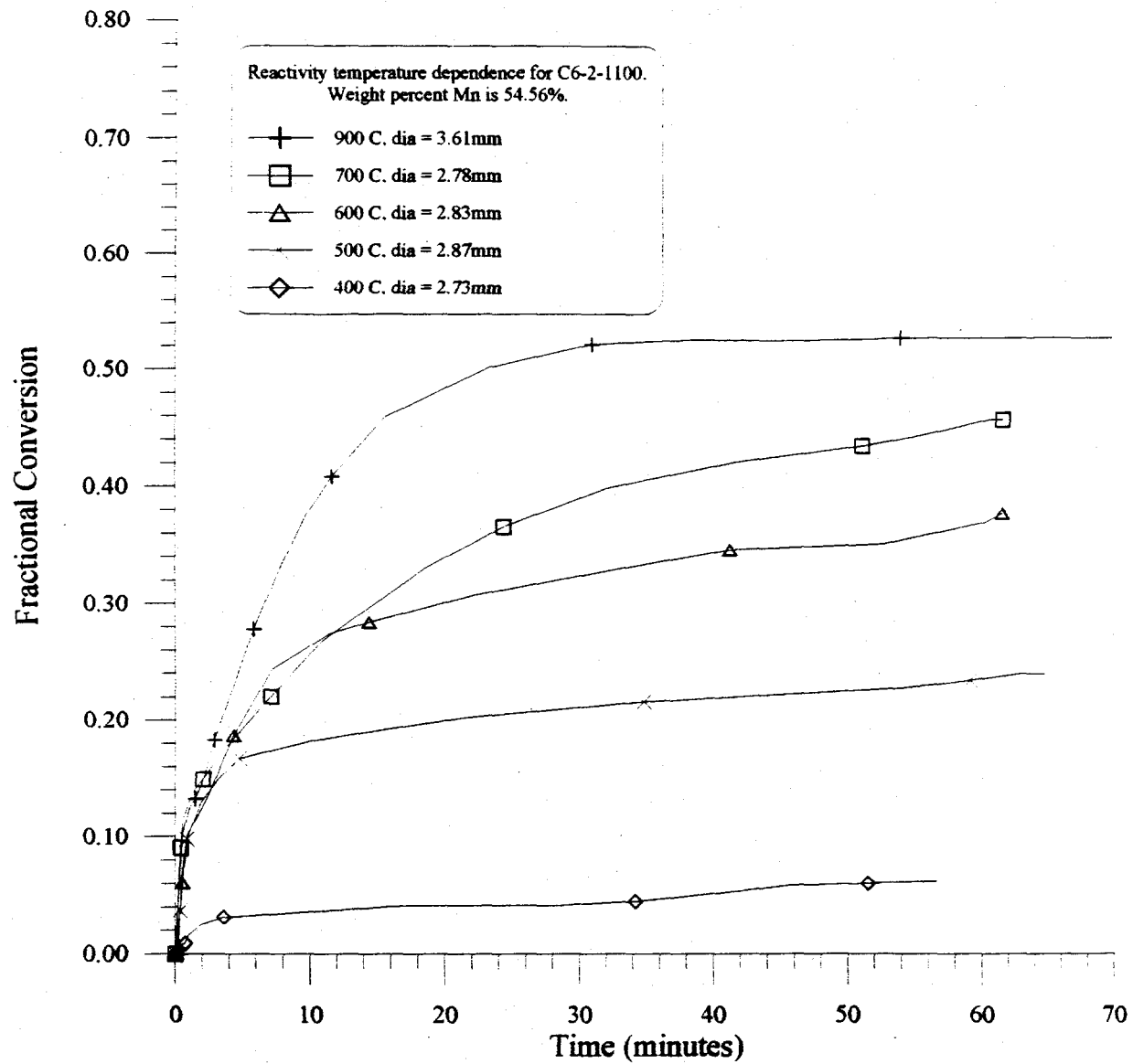


Figure 9. Effect of temperature on pellet reactivity for C6-2-1100.

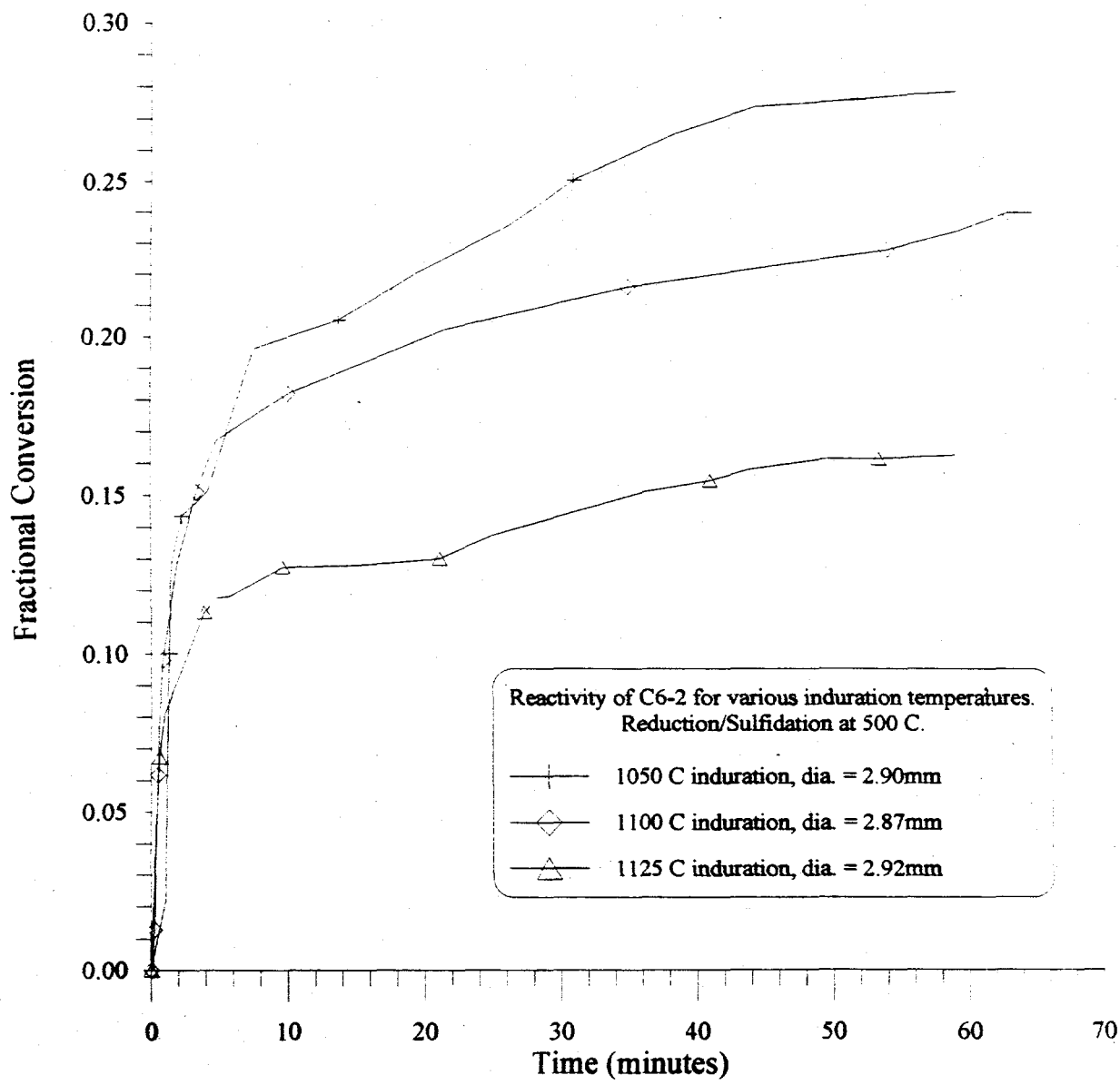


Figure 10. Effect of induration temperature on sulfidation conversion at 500 °C, for C6-2-XXXX.

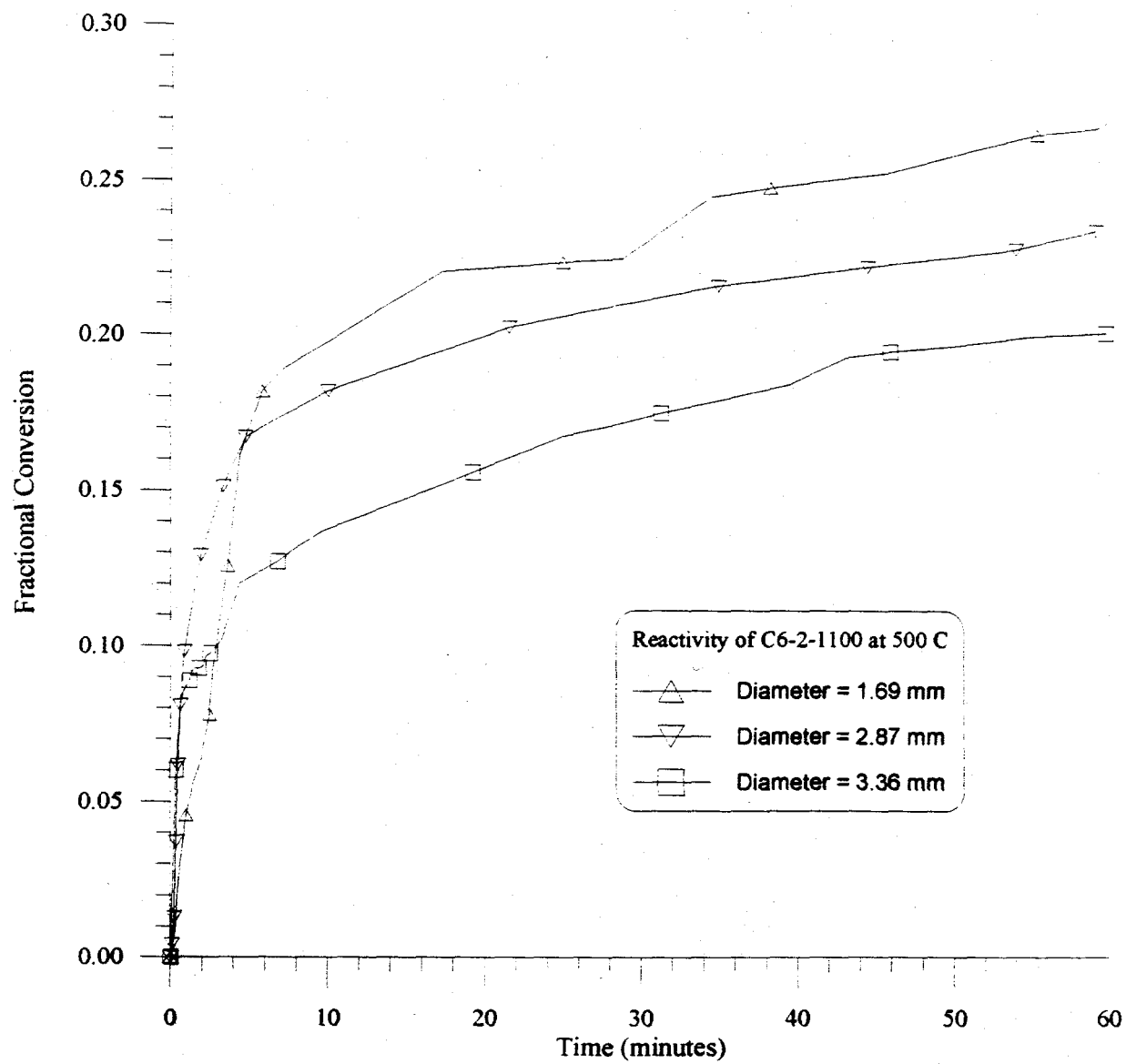


Figure 11. Effect of pellet diameter on sulfidation conversion at 500 °C, for C6-2-1100.

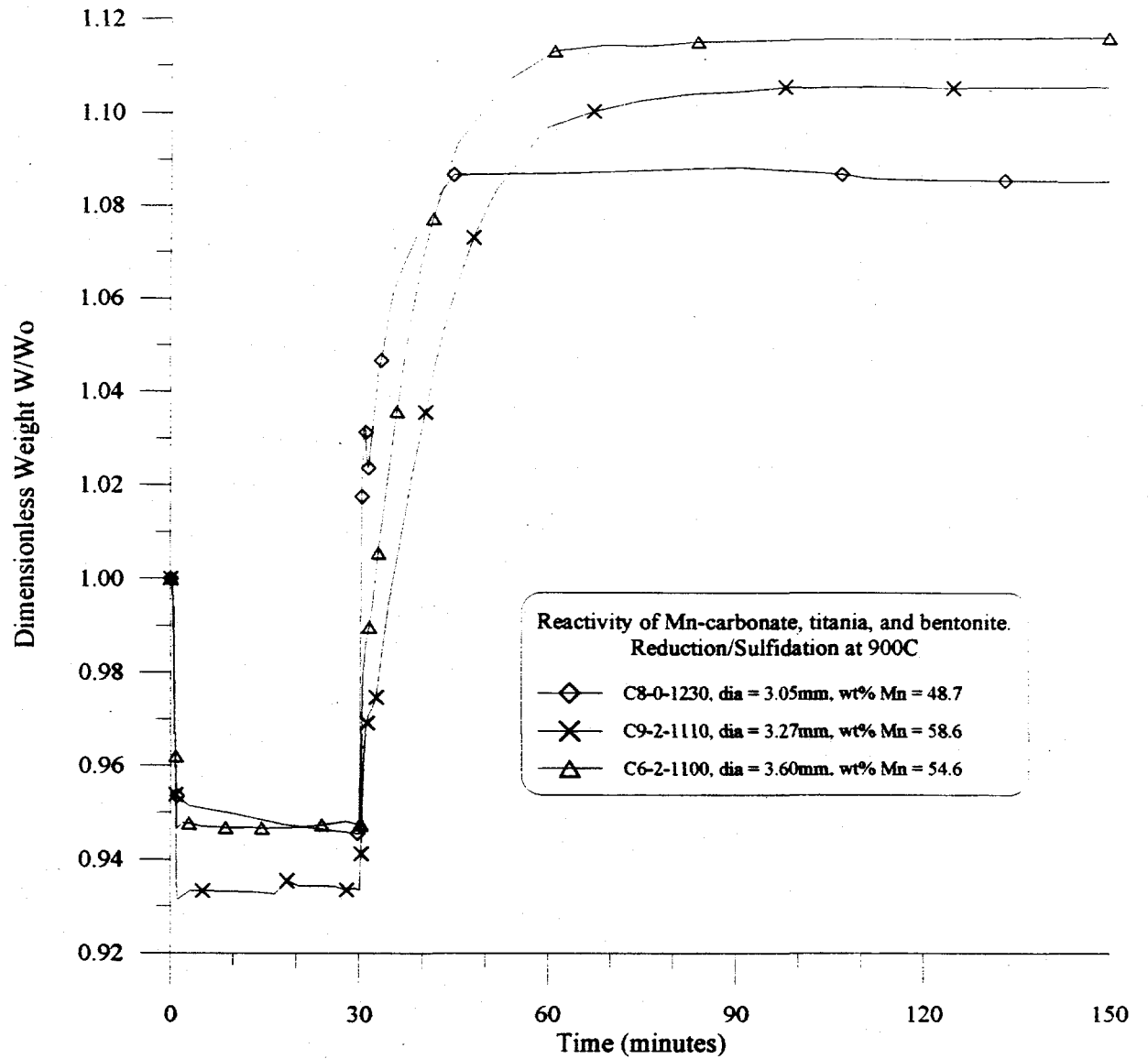
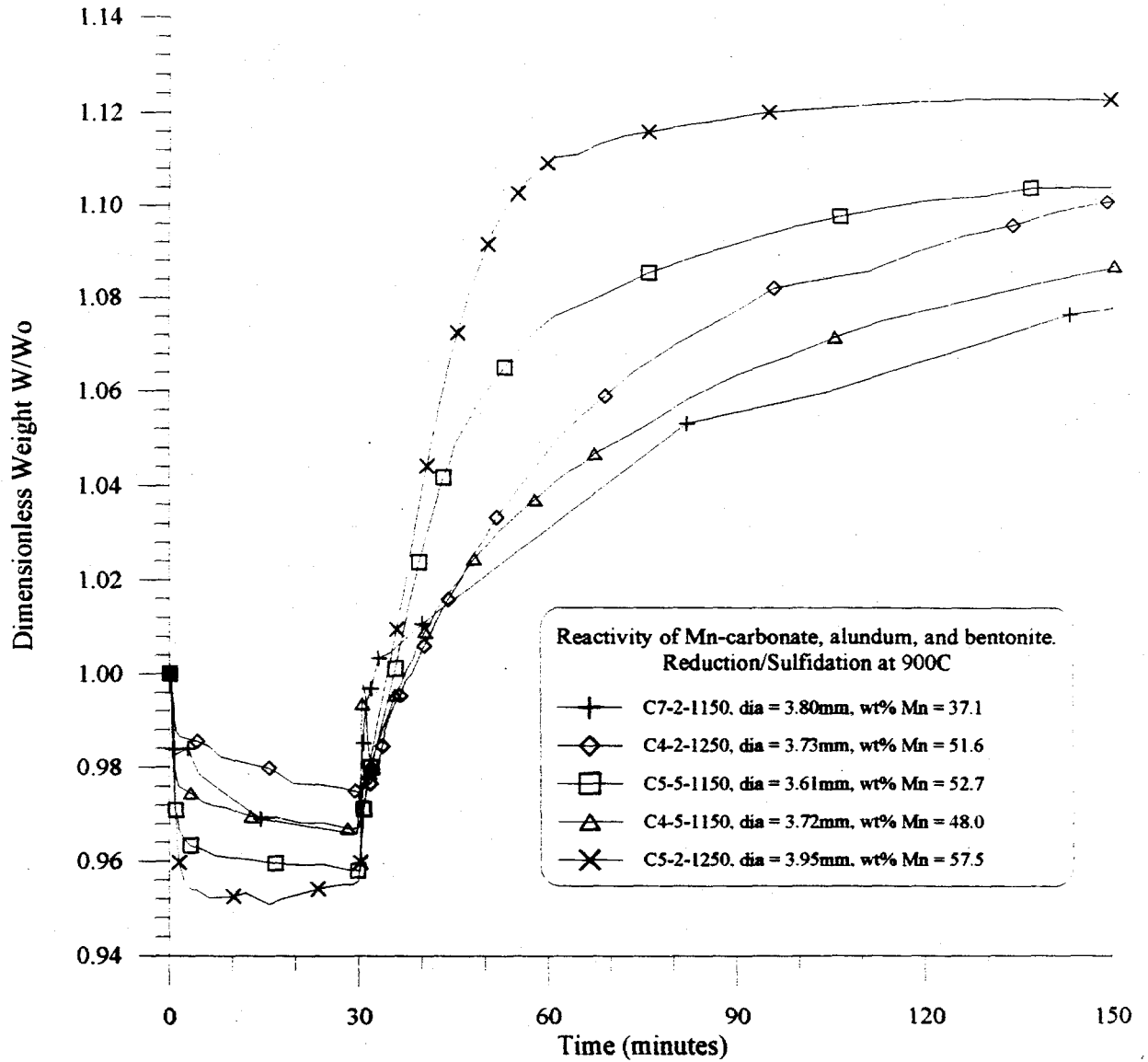
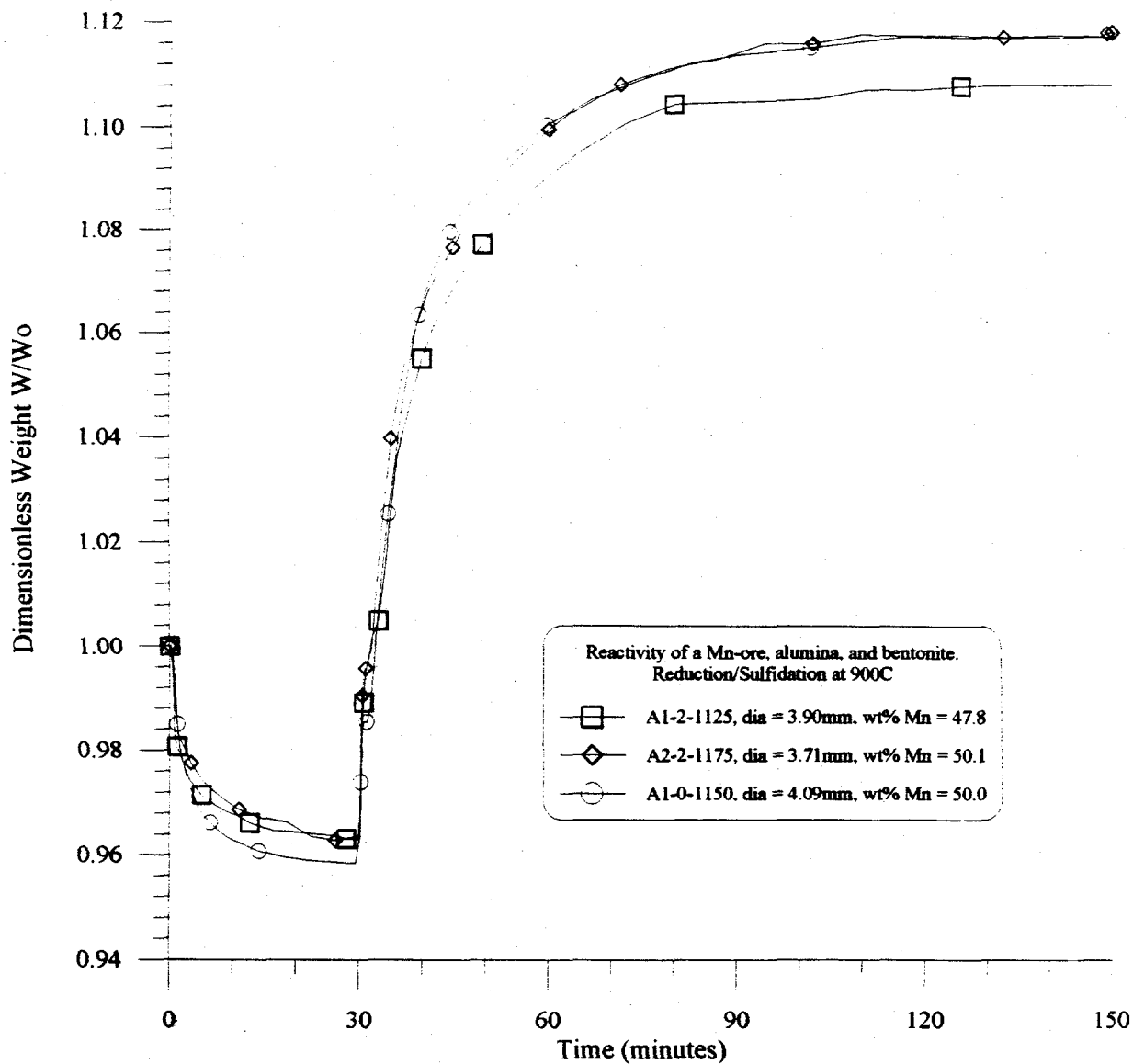


Figure 12. Pellet reactivity at 900 °C, for Mn-carbonate based, Titania supported formulations.



**Figure 13.** Pellet reactivity at 900 °C, for Mn-carbonate based, Alundum supported formulations.



**Figure 14.** Pellet reactivity at 900 °C, for Mn-ore based, Alundum supported formulations.

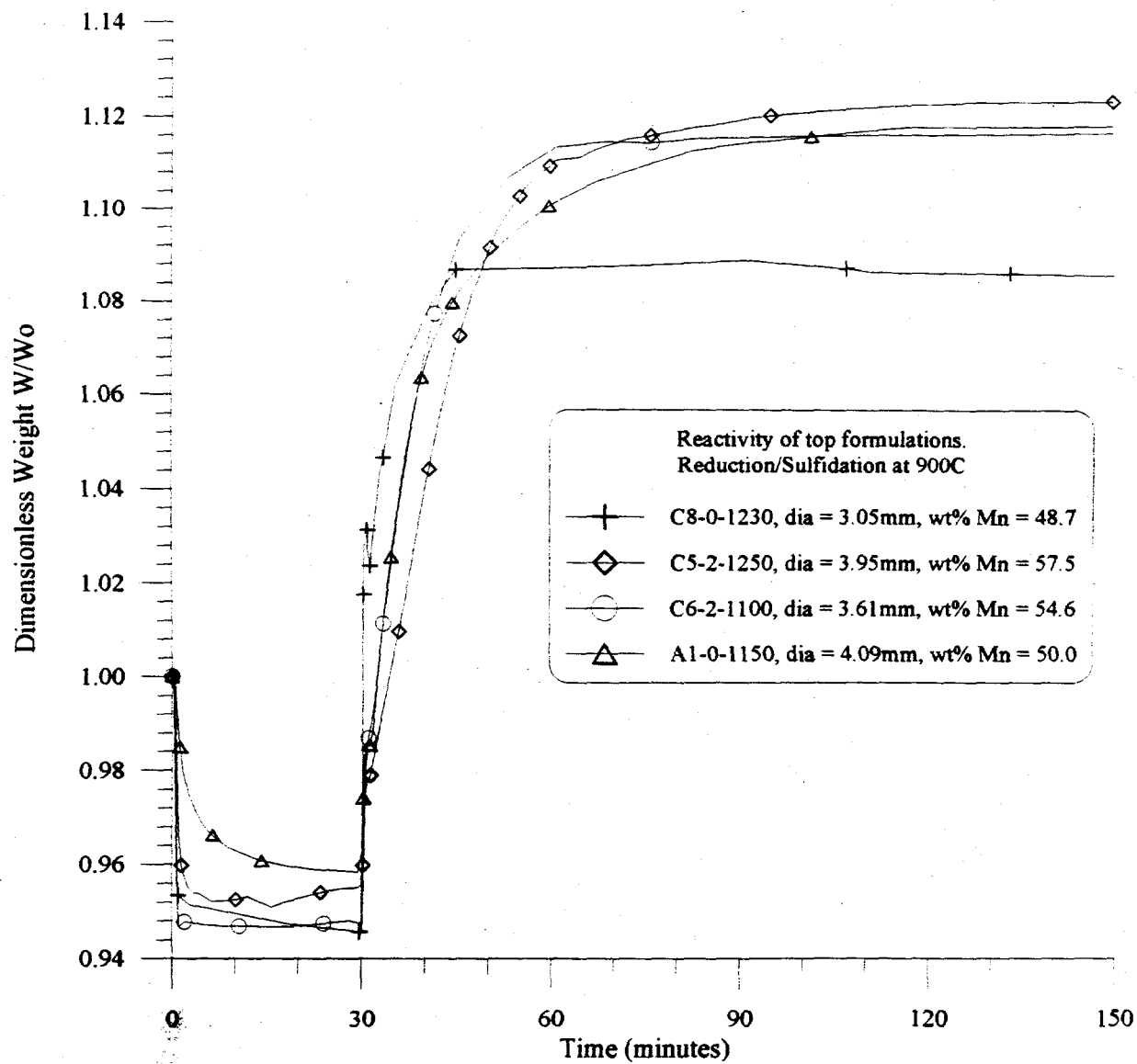


Figure 15. Pellet reactivity at 900 °C for selected formulations.

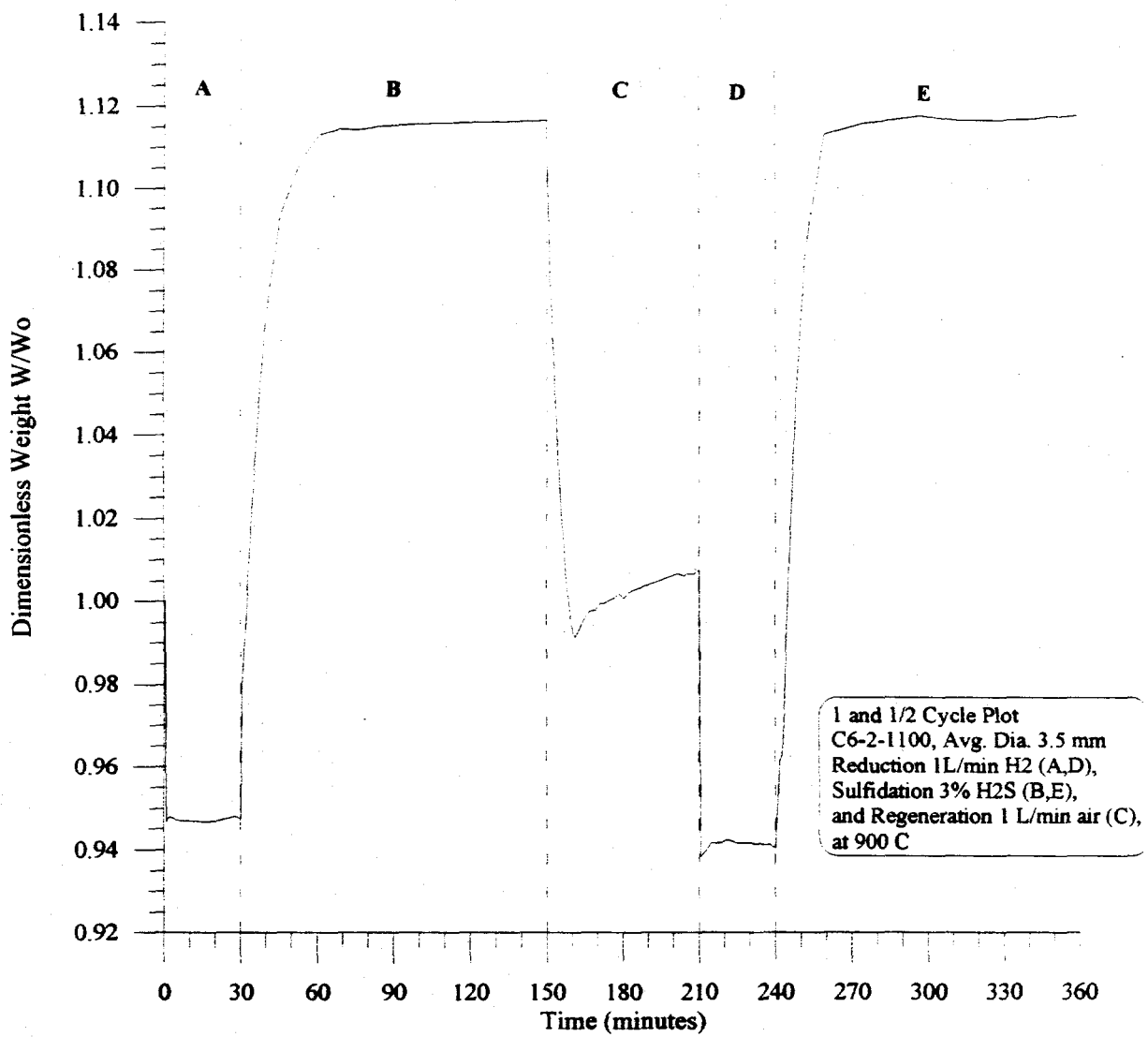


Figure 16. 1 and 1/2 cycle plot at 900 °C for C6-2-1100.

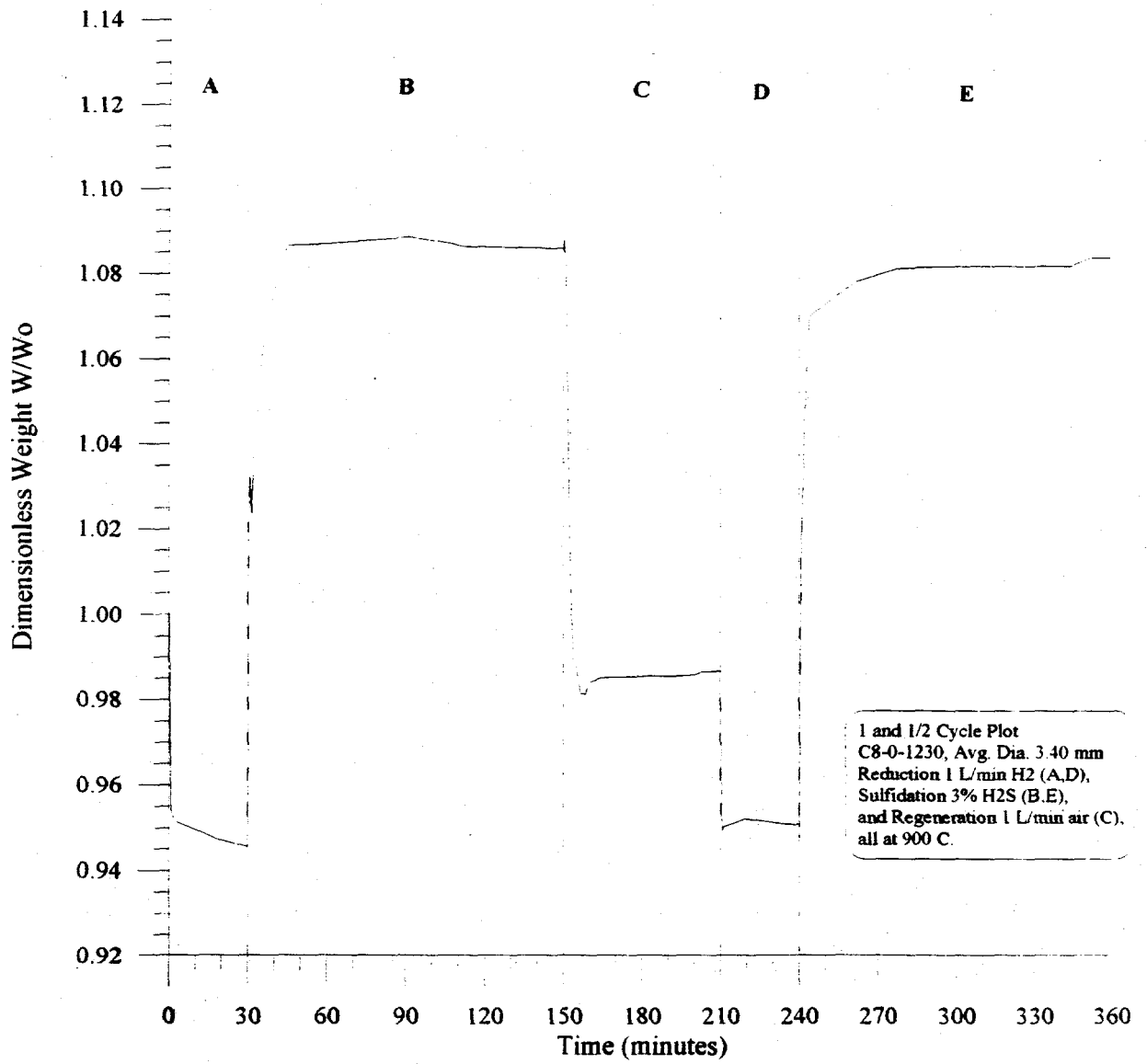


Figure 17. 1 and 1/2 cycle plot at 900 °C for C8-0-1230.

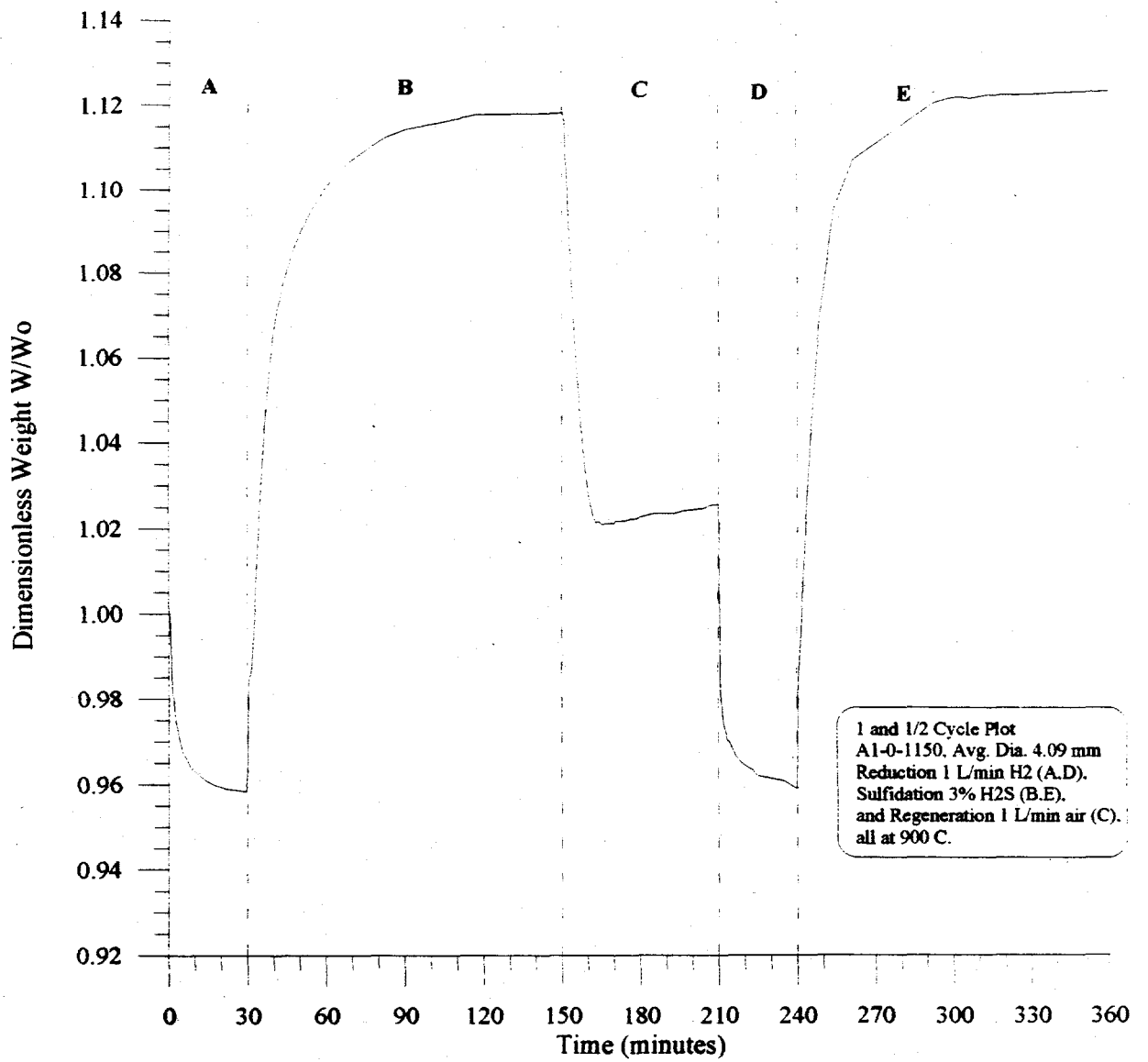


Figure 18. 1 and 1/2 plot at 900 °C for A1-0-1150.